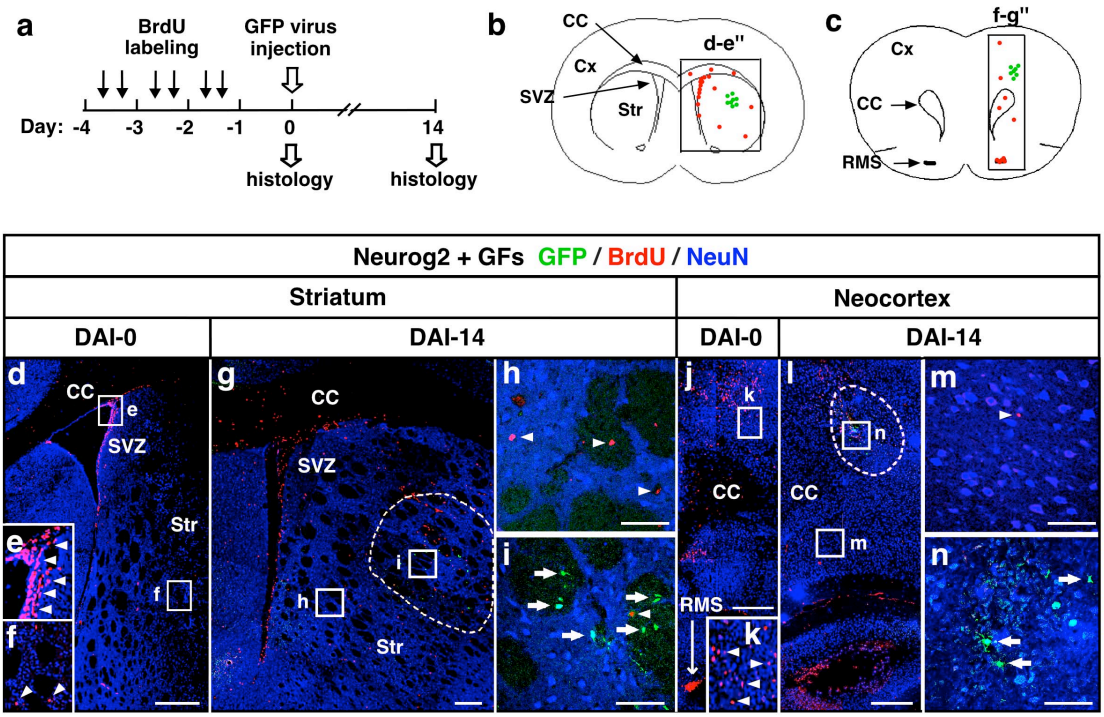

Supplementary Figure S1. Differential labeling of SVZ and parenchymal cells with BrdU and GFP retroviruses. (a) Schematic diagram illustrating the time course of BrdU labeling and virus infection. (b, c) Schematic diagrams showing the topological relationship between $BrdU^+$ and GFP^+ cells 14 days after striatal (b) and cortical (c) injection. (d-n) Distribution patterns of $BrdU^+$ and GFP^+ cells in the striatum (d-i) and neocortex (j-n). The sections were triple-stained for BrdU (red) (arrowheads), GFP (green) (arrows), and NeuN (blue). Dashed circles in g and l indicate the areas of virus infection. Scale bar: d, e, f, g, 500 μm; and h, i, m, n, 50 μm.

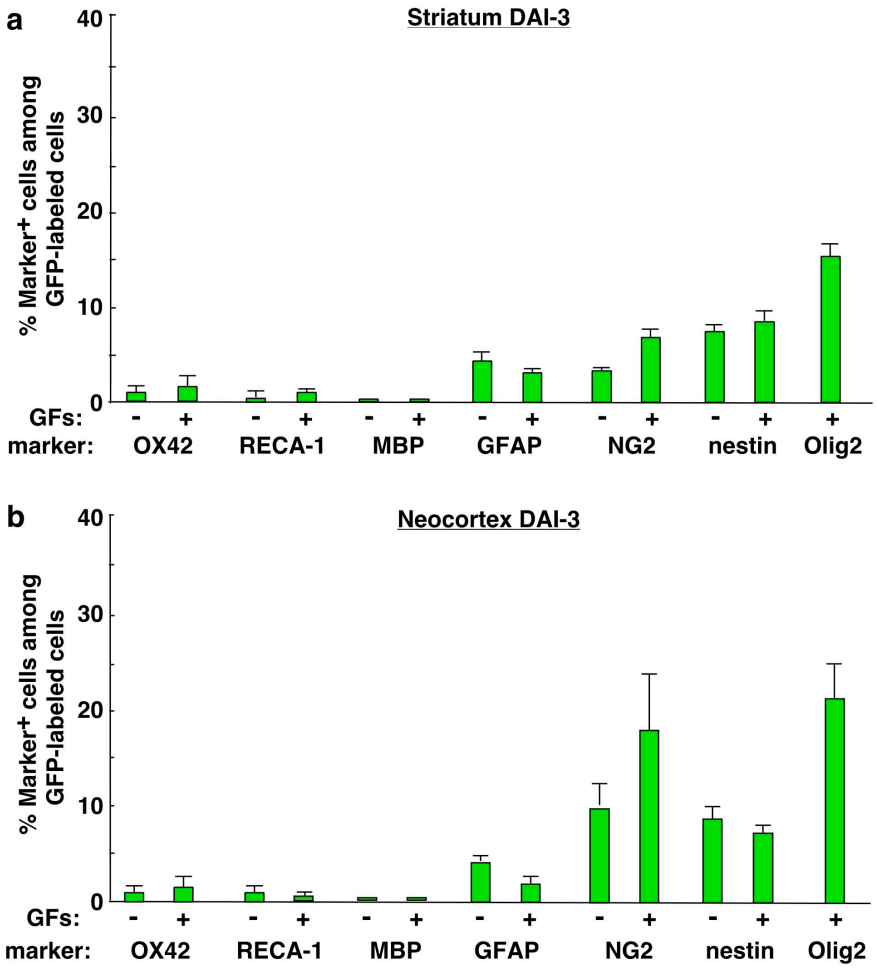

Supplementary Figure S2. Phenotypes of control retrovirus-infected cells early after infection. Co-expression of various cell type-specific markers in GFP$^+$ cells was examined in the striatum (a) and neocortex (b) at DAI-3. Graphs show the percentages of cells expressing various markers (shown at the bottom) among total GFP$^+$ cells in the presence (+) or absence (-) of GFs. Data are mean $\pm$ s.d. (n = 3 animals). Note that the very low percentages of OX42$^+$ and GFAP$^+$ cells among GFP$^+$ cells in both regions are probably because viruses were injected into the intact brain where resident microglia and astrocytes were mostly quiescent. Since the infectablility of viruses is lost very rapidly in vivo, only cells that enter the cell cycle during a short period after virus injection are labeled.

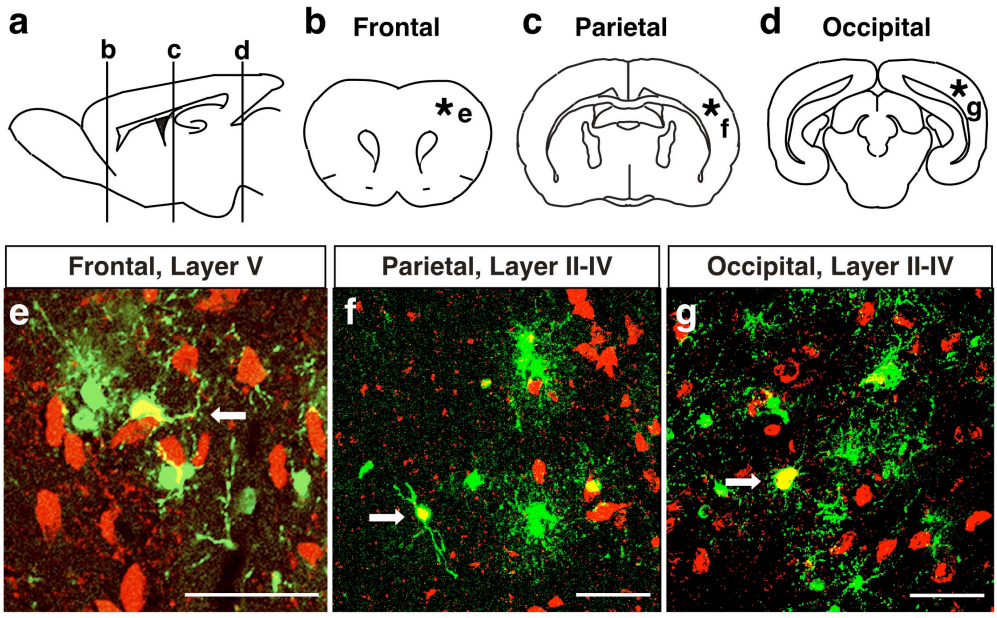

Supplementary Figure S3. Induction of GFP$^+$/NeuN$^+$ cells by Neurog2/GF-treatment in various neocortical areas. (a) A schemiatic parasagittal view of the adult brain in which approximate locations of the coronal sections shown in b-d are indicated by vertial lines. (b-d) Schemiatic representations of the coronal sections of the adult brain at different anteroposterior levels. Asterisks indicate the areas where GFP$^+$/NeuN$^+$ cells (arrows) in e-f were detected at DAI-14 after injection of Neurog2 viruses and GFs. Scale bar: 50 μm.

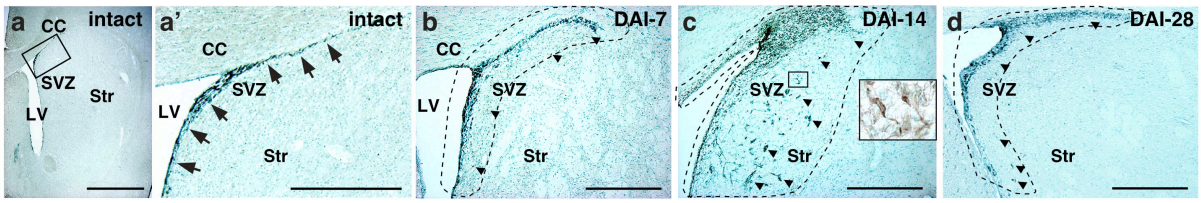

Supplementary Figure S4. Upregulation of neurogenesis in the SVZ after cortical ischemia. The distribution patterns of Dcx^+ new neurons cells in the intact and ischemic brain are compared. Box in a indicates the location of the areas shown in a'-d. Arrows in a' indicate Dcx^+ cells confined to the SVZ of the intact brain. Dashed lines in b-d indicate the areas in which Dcx^+ cells (arrowheads and inset in c) are dispersed beyond the border between the SVZ and adjacent striatum. Scale bar: a, 2 mm; and a'-d, 400 mm.

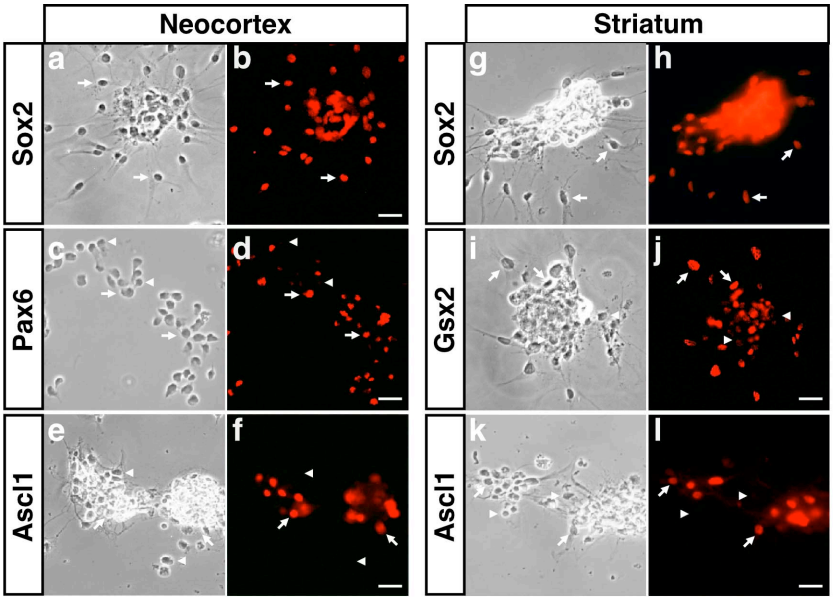

Supplementary Figure S5. Expression of specific transcription factors in NPC-like cells derived from the adult neocortex and striatum. Neurospheres grown from the neocortex (a-f) and striatum (g-l) are stained for the proteins indicated on the left. a, c, e, g, i, and k show phase-contrast images, and b, d, f, h, j, and l show immunofluorescent images of the same visual fields. Arrows and arroheads indicate immuno-positive and -negative cells, respectively. Note that Sox2 is expressed most cells in both the neocortex and struatum,

Supplementary Table S1. Estimated total numbers of virus-infected GFP$^+$ cells per hemisphere under various conditions. The conditions compared are shown on the top (+, present; -, absent), and time points examined are shown on the left. Data are mean ± s.d. (n = 3-4 animals). nt, not tested.

Condition		Estimated number of total GFP$^+$ cells per hemisphere					
Stab wound		+	+	+	+	+	+
Growth factor treatment		-	+	-	+	+	+
Neurog2 overexpression		-	-	+	+	-	+
Ischemic injury		-	-	-	-	+	+
Striatum	DAI-3	15,420±851	21,342±902	10,030±781	14,844±828	nt	nt
	DAI-7	5,620±391	6,663±313	5,122±496	6,534±596	6,830±240	7,201±410
	DAI-14	5,146±792	6,405±475	4,520±1,008	6,640±682	6,321±717	6,900±705
	DAI-28	nt	3,102±131	2,897±254	3,685±1,132	nt	nt
	DAI-56	nt	nt	nt	3,525±205	nt	nt
	DAI-84	nt	nt	nt	3,200±156	nt	nt
Neocortex	DAI-3	16,775±2,496	80,257±3,299	9,784±1,025	31,462±3,687	133,547±27,774	50,988±7,795
	DAI-7	nt	24,952±4,506	5,825±431	21,053±3,109	74,943±5,151	37,640±3,408
	DAI-14	8,052±973	17,350±1,917	5,211±1,353	16,230±2,342	20,010±4,732	17,500±2,715
	DAI-28	nt	12,491±2,506	nt	13,309±289	nt	nt
	DAI-56	nt	nt	nt	10,266±1,091	nt	nt

Supplementary Table S2 Antibodies used for immunostaining.

Antigen	Species	Source	Catalog #	Condition	Reference
MAP2	Rabbit	Y. Ihara, University of Tokyo	-	1:500	1
Nestin	Rabbit	In-house	-	1:1,000	1
Nestin	Mouse	Developmental Studies Hybridoma Bank of the University of Iowa	Rat 401	1:500	
Olig2	Rabbit	In-house	-	1:3,000	2
Neurog2	Rabbit	Santa Cruz Biotechnology	sc-19233	1:100	2
Ascl1	Rabbit	In-house	-	1:1,000	2
Ascl1	Mouse	BD Pharmingen	556604	1:200	
Pax6	Rabbit	In-house	-	1:1,000	2
Bhlhb5	Goat	Santa Cruz Biotechnology	SC-6045	1:200	
GFP	Rabbit	Invitrogen	A-11122	1:5,000	
GFP	Rat	Nakarai-Tescqu	04404-84	1:5,000	
BrdU	Rat	Oxford Biotechnology	OBT0030	1:1,000	
NeuN	Mouse	Millipore	MAB377	1:1,000	
Dcx	Goat	Santa Cruz Biotechnology, Inc.	sc-8067	1:200	
TuJ1	Mouse	Babco	MMS-435P	1:5,000	
HuC/D	Mouse	Invitrogen	A21271	1:1,000	
GABA	Rabbit	Sigma-Aldrich	A2052	1:1,000	
DARPP-32	Rabbit	Millipore	AB1656	1:1,000	
Calretinin	Rabbit	Millipore	AB149	1:2,000	
Calbindin D-28k	Rabbit	Millipore	AB1778	1:500	
Parvalbumin	Mouse	Millipore	MAB1572	1:1,000	
Glutamate	Mouse	Sigma-Aldrich	G9282	1:1,000	
Glutamate	Rabbit	Sigma-Aldrich	G6642	1:5,000	
GluR2/3	Rabbit	Millipore	AB1506	1:200	
GFAP	Mouse	Millipore	MAB360	1:2,000	
GFAP	Rouse	Millipore	AB5804	1:1,000	
NG2	Mouse	Millipore	MAB5384	1:500	
Myelin basic protein	Mouse	Millipore	MAB382	1:1,000	

O4	Mouse	Millipore	MAB375	1:300	
OX42	Mouse	Serotec	MCA275R	1:1,000	
RECA1	Mouse	Serotec	MCA970	1:5	
Synaptophysin	Mouse	Roche	MAB5258-20UG	1:00	
FG	Rabbit	Millipore	AB153		

Supplementary Table S3 Primers used for qRT-PCR analysis

Gene	Sense Primer	Antisense Primer
Ascl1	5’-AGATGAGCAAGGTGGAGACG-3’	5’-TGGAGTAGTTGGGGGAGATG-3’
Emx2	5’-TCAGAACCGGAGAACGAAAT-3’	5’-TCTCCACCGGTTAATGTGGT-3’
GAPDH	5’-ACCACAGTCCATGCCATCAC-3’	5'-TCCACCACCTGTTGCTGTA
Gsx2	5’-CCTTTGCTCAAAAGCCAGTT-3’	5’-GGTGATGGTGATGATGATGC-3’
Neurog2	5’-ACCGCATGCACAACCTAAAC-3’	5’-AGCGCCCAGATGTAATTGTG-3’
Pax6	5’-CGGAGGGAGTAAGCCAAGAG-3’	5’-TCTGTCTCGGATTTCCCAAG-3’
Six3	5’-GAAGAGTTGTCCATGTTCCA-3’	5’-ATCGACTCGTGTTTGTTGAT-3’
Sox2	5’-CACAGATGCAACCGATGCA-3’	5’-GGTGCCCTGCTGCGAGTA-3’

Supplementary References

61) Torii M, Matsuzaki F, Osumi N, Kaibuchi K, Nakamura S, Casarosa S, Guillemot F, Nakafuku M. Transcription factors Mash-1 and Prox-1 delineate early steps in differentiation of neural stem cells in the developing central nervous system. *Development* **126**, 443-456 (1999).

62) Mizuguchi R, Sugimori M, Takebayashi H, Kosako H, Nagao M, Yoshida S, Nabeshima Y, Shimamura K, Nakafuku M. Combinatorial roles of Olig2 and Neurogenin2 in the coordinated induction of pan-neuronal and subtype-specific properties of motoneurons. *Neuron* **31**, 757-771 (2001).